Low-Velocity Impact Behavior of Carbon/Basalt Fiber-Reinforced Intra-ply Hybrid Composites

Article *in* Iranian Journal of Science and Technology: Transactions of Mechanical Engineering · February 2018
DOI: 10.1007/s40997-018-0151-3

2 authors:

Farzin Azimpour shishevan
Ataturk University
16 PUBLICATIONS **4** CITATIONS
SEE PROFILE

H. Akbulut
Ataturk University
43 PUBLICATIONS **180** CITATIONS
SEE PROFILE

Iran J Sci Technol Trans Mech Eng
https://doi.org/10.1007/s40997-018-0151-3

RESEARCH PAPER

Low-Velocity Impact Behavior of Carbon/Basalt Fiber-Reinforced Intra-ply Hybrid Composites

Farzin Azimpour Shishevan[1] · Hamit Akbulut[1]

Received: 7 February 2017 / Accepted: 5 February 2018

Abstract
The effect of hybridization on the low-velocity impact behavior of woven carbon/basalt fiber-reinforced intra-ply hybrid composites was investigated experimentally. Three types of basalt- and carbon-based homogeneous with 60% volume fraction of neat fiber (basalt fiber and carbon fiber) and twill intra-ply hybrid composite laminates with 30 wt% carbon and 30 wt% basalt fiber contents were fabricated by vacuum-assisted resin infusion molding method. Improvement in the impact toughness and reduction in the cost of carbon fiber-reinforced polymer (CFRP) composites were the main purposes of using this type of hybrid composites. Energy profile method was used to determine the impact penetration threshold. In this regard, drop weight tests are carried out in 20, 50, 60 and 80 J energy magnitudes and force–deflection and absorbed energy–time diagrams are plotted. The effect of intra-ply hybridization on maximum contact force, absorbed energy, maximum deflection and duration time of carbon/basalt-based composites was investigated. According to the scanning electron microscopy results, various failure modes occurred during low-velocity impact test such as micro-cracks, debonding, delamination in interface, fiber pull out and fiber breakage. The results indicate that the impact performance of homogenous composites is improved by hybridization, i.e., the maximum force and absorbed impact energy of CFRPs are increased 62.3 and 186% by the addition of basalt fibers as a complementary element to the structure of composites.

Keywords Low-velocity impact · Intra-ply hybrid · Basalt fiber · Carbon fiber

1 Introduction

Nowadays, the use of carbon fiber-based polymer composites has become widespread in aeronautic and automotive industries, not only because of their good mechanical and thermal properties but also their lightness that ensures energy saving (Muñoz et al. 2014). Continuous usage of polymer matrix composites led to further development of these materials. Hybrid composite as a new generation can provide flexibility in the use of these materials by employing various fiber types in the structure of composite to obtain the desired properties according to working conditions. The hybrid composites are available in two types as inter-ply and intra-ply. In inter-ply type, the structure of composite consists of the stacked plies where each ply includes one type of reinforcements and the reinforcement material may be changed in different plies. On the other hand, in the intra-ply hybrid type two or more types of reinforcements are used in each ply while the same fiber/matrix system was used for the whole plies (Sarasini et al. 2013a).

Fabricated composite materials may be exposed to the various unwanted loadings during the application process. Low-velocity impact load is one the most common types of loadings that happens consecutively when using the composites. Hence, improvement in the impact behavior of composites has gained high importance.

As known, carbon fibers are commonly used in the structure of polymer composites because of their superior mechanical and thermal properties (Han et al. 2013). However, the weakness of these fibers against impact loads because of low toughness and their high price has restricted their widespread application (Akangah et al. 2010; Czigany

✉ Farzin Azimpour Shishevan
fazimpoor@gmail.com

Hamit Akbulut
akbuluth@atauni.edu.tr

[1] Department of Mechanical Engineering, Ataturk University, Erzurum, Turkey

Published online: 28 February 2018

2006; Sarasini et al. 2014). Recently, some of the fiber types such as glass, (Imielinska and Guillaumat 2004; Pegoretti et al. 2004) and nylon fibers (Akangah et al. 2010; Tehrani-Dehkordi et al. 2015) have been used as a hybridization component with carbon fiber to improve the toughness and reduce the price of fabrication. On the other hand, low price and environment-friendly behavior of natural fibers such as bamboo (Nayak et al. 2009), hemp (Petrucci et al. 2013), coir (Rout et al. 2001) and basalt (Carmisciano et al. 2011; Liu et al. 2006; Wei et al. 2010, 2011) as an alternative component in the structure of CFRP has widely spread. However, low mechanical and thermal properties and high hydrophilic nature of most of these natural fibers have restricted their applications in industry. Among these, the basalt fiber is an appropriate option for hybridization with carbon fibers due to good mechanical properties such as higher Young modulus (Liu et al. 2006), flexural strength (Szabo and Czigany 2003), good toughness (Zhang et al. 2009), superior thermal properties, low price because of extensive resource (Fiore et al. 2011) and no need of any additives in the manufacturing process (Carmisciano et al. 2011; Fiore et al. 2015). Furthermore, nontoxicity (Mcconnell et al. 1994) and durability of this type of fibers to acidic (Sim et al. 2005) and alkali (Ramachandran et al. 1981) conditions make them the best candidate for hybridization with other fiber types.

The effects of hybridization and temperature change on the low-velocity impact behavior of hemp/basalt hybrid composites were investigated by Kumar et al. (2015). Chandekar and Kelkar (2014) studied the low-velocity impact behavior of homogenous carbon, basalt and inter-ply hybrid of these fiber-reinforced composites. The effect of hybridization on the drop weight impact behavior of woven carbon/aramid composites has been studied by Karahan and Karahan (2014). Post-impact mechanical characterization of glass and basalt fiber-reinforced homogenous composite materials was studied by Rosa et al. (2012). Better post-impact mechanical behavior of BFRP than E-glass fiber-reinforced composites is as a result of this research. Low-velocity impact behavior of aramid/basalt inter-ply hybrid composites has been investigated by Sarasini et al. (2013a). They stiffed thirteen laminates of basalts and aramids in the configuration of seven basalt laminates as a core and three aramid-reinforced laminates in each side of the sandwich-based structure. In another research led by Sarasini et al. (2013b), glass fiber has been hybridized with basalt fiber and the low-velocity impact behavior of these inter-ply hybrid composites has been studied. The results of this research indicated that the impact behavior of inter-ply hybrid composite was severely affected by the stacking sequence of laminates. Furthermore, it is very hard to find the optimum stacking sequence of these composites for bearing various loading conditions with sufficient safety factor. On the other hand, in the intra-ply hybrid composites in which all constituent laminates structures are similar, the stacking sequence does not affect the counteraction of composites under different loading conditions. Moreover, the toughness of intra-ply hybrid composites is more than the inter-ply and this leads to a better impact performance (Tehrani-Dehkordi et al. 2015). The low-velocity impact behavior of basalt/nylon-based intra-ply hybrid and homogenous composites has been studied by Tehrani-Dehkordi et al. (2015). Combination of good mechanical properties of basalt fibers with superior impact behavior of nylon fibers has been reported as the purpose of this research. The results of this research show that intra-ply hybrid composites exhibited better tensile properties and impact behavior than inter-ply ones. As seen above, various researches have studied the effects of inter-ply hybridization on low-velocity impact behavior of composite materials. However, few researches have been carried out on the intra-ply hybridization effect. In this research, the effects of intra-ply hybridization on the low-velocity impact behavior of carbon and basalt fiber-reinforced composites are studied. For this purpose, three types of carbon and basalt fibers reinforced with homogeneous and intra-ply hybrid composites are fabricated and exposed to various energy low-velocity impact tests. Energy calibrations are carried out using energy profile method, and penetration threshold of CFRP, basalt fiber-reinforced polymer (BFRP) and carbon/basalt fiber-reinforced polymer (CBFRP) intra-ply hybrid composites is determined. Contact load–deflection and energy–time diagrams are drawn for various impact energies, and the maximum impact force, maximum deflection, absorbed energy and contact duration time are compared.

2 Experimental Procedure

2.1 Materials and Specimen Preparation

2.1.1 Intra-ply Hybrid Composite Fabrication

Three types of 2/2 woven textiles were used in the structure of fabricated composites. Two textiles were made up from neat carbon and basalt fibers. In the third textile, carbon and basalt fibers were woven together, creating intra-ply hybrid fabrics. As was mentioned, intra-ply hybrid composites consist of plies by the same reinforcement structure that was stacked up. Woven intra-ply hybrid fabrics include woven textile in which basalt and carbon threads were woven together in twill 2/2 pattern, and each thread consists of 1200 yarn filaments. This pattern is identified by its

diagonal parallel lines known as wales. Designated 2/2 numerator indicates two threads of carbon fiber as weft thread must pass over two basalt threads as warp and then under two other basalt threads. The schematic and weaved intra-ply CBFRP hybrid composite is shown in Fig. 1a, b.

Three types of homogenous and hybrid composites that include carbon and basalt fibers were fabricated by using vacuum-assisted resin infusion molding (VARIM) method (Fig. 1). The encoding, percentage of components for each type and thickness of samples are given in Table 1. The carbon and basalt fibers were purchased and woved in Spinteks Textile Co., Denizli, Turkey. The weaving of intra-ply hybrid textile that includes carbon and basalt fiber in the same layer occurred in twill tip. In this type of pattern, carbon and basalt fibers were woven in 0 and 90° orientation angles (Fig. 1b).

Huntsman Araldite 1564/Aradur 3487 epoxy were used as the matrix of composites mixed with its hardener (Aradur 3487) and prepared from Huntsman Advanced Materials, USA (Fig. 2). Fabrication of composites was carried out in Fibermak composites Ltd. CO., Izmir, Turkey. As seen in Fig. 3a, the curing process of the composites was carried out at − 1 atm pressure and 80 °C for 8 h. The VARIM setup is shown in Fig. 3b.

Homogenous and hybrid composite plates were fabricated in the dimensions of 700 × 700 mm^2 consisted of 24 intra-ply hybrid laminates (Fig. 3c). Composite plates were cut with water jet in the size of 100 × 100 mm^2 as low-velocity impact sample according to ASTM D 7136.

2.2 Low-Velocity Impact Test

Low-velocity impact test is performed in Composite Research Laboratory of Mechanical Engineering Department in Dokuz Eylül University, Turkey. The Fractovis Plus impact test machine is used as the low-velocity impact testing instrument. This instrument is appropriate for testing in various impact energy magnitudes, and it uses software that is able to apply time-dependent force and to calculate impact velocity, deflection and energy. The maximum load capacity of the instrument is 22.4 kN. The hole diameter of the pneumatic specimen fixture is 76.2 mm. The used impactor has a hemispherical nose with the diameter of 12.7 mm and the mass of 4.906 kg.

3 Results and Discussion

Three types of responses may occur during the impact test including the rebounding, penetration and perforation. In the rebounding, energy of impactor is not enough to penetrate to the surface of specimen and the impactor gives the amount of its energy to specimen and damages it during contact with the surface of specimen. As a result, the velocity of the impactor is reduced and vanishes temporarily and changes its movement direction. In penetration, the energy of impactor is enough for penetrating into the specimen. Thus, after the impactor contacts with the surface of the specimen, the velocity of the impactor starts to decrease and becomes zero, same as the rebounding. Total energy of the impactor is absorbed by specimen and impactor gets stuck in the specimen. During the perforation, the energy of impactor is not only enough for penetration, but also it is sufficient for perforating the specimen. During the perforation, some of the impact energy is consumed by the friction between the impactor and the perforated specimen.

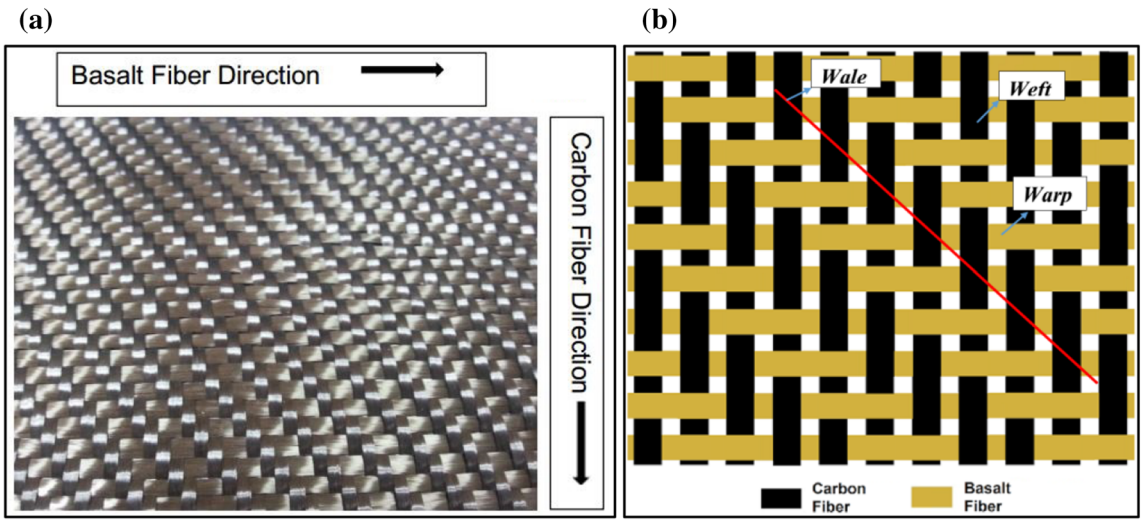

Fig. 1 **a** Intra-ply hybrid fabric, **b** schematic of weaved 2/2 twill CBFRP intra-ply hybrid fabric, carbon/basalt intra-ply hybrid fabric

Table 1 Encoding, component percentage and thickness of fabricated composites

Material	Encoding	Carbon fiber (%)	Basalt fiber (%)	Epoxy (%)
Carbon/epoxy (CFRP)	C	60	0	40
Basalt/epoxy (BFRP)	B	0	60	40
Carbon/basalt/epoxy (CBFRP)	CB	30	30	40

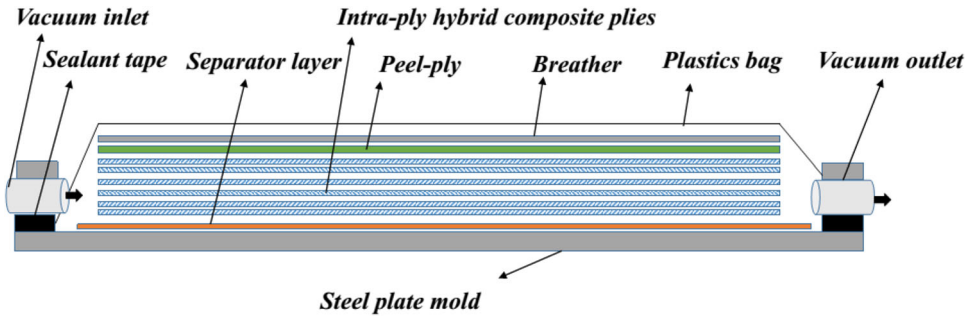

Fig. 2 Schematic of VARIM method

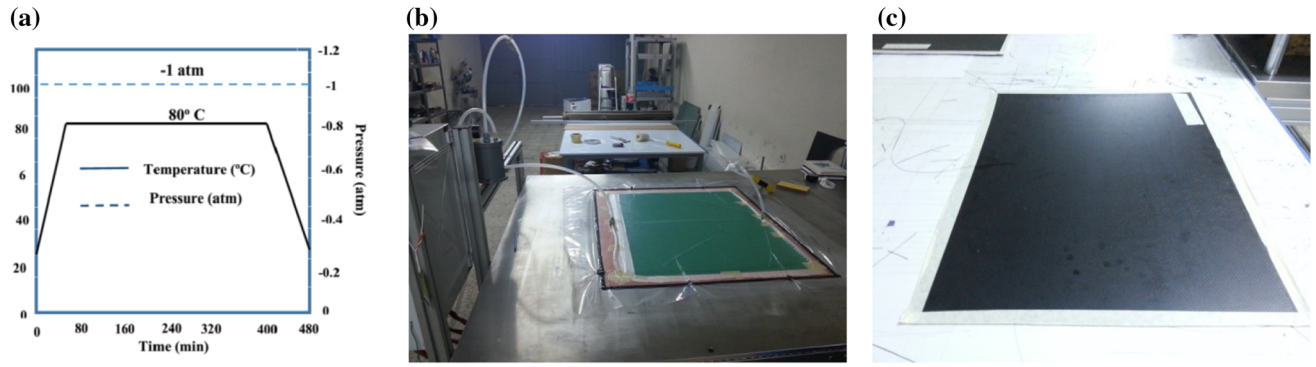

Fig. 3 Manufacturing process of homogenous and hybrid composites, **a** schematic of curing process, **b** VARIM method, **c** fabricated CBFRP intra-ply hybrid plate

In order to investigate the effect of hybridization on the low-velocity impact behavior of the laminated composite materials which are reinforced with carbon and basalt fibers, the impact tests are performed at various energies (Icten et al. 2009). For this purpose, until reaching the perforation threshold, the magnitude of the impact energy is continuously increased and the magnitude of absorbed energy versus impact energy is identified in the equal energy diagram. This diagram includes a diagonal line that is named energy line. Position of the registered point for each impact test describes the status of the tests. Three statuses may show up depending on the position of the energy point. In the first status, the energy point is located under the equal energy line. In this manner, the magnitude of absorbed energy is less than the impact energy and the impactor energy is insufficient to penetrate the specimen, thus, the impactor is rebounded from the surface of the specimen. In this condition, the difference between impact and absorbed energy magnitude is named as rebounding energy and the energy point is located under the equal energy line. During rebounding, the sum of rebounding and absorbed energies is equal to the impact energy. In the second status, magnitude of the impact energy is higher from the first status. In this status, the energy point is located on the equal energy line, that is, the impact energy magnitude is equal to the absorbed energy. In this manner, the whole impact energy of impactor is absorbed by specimen and impactor penetrates into the specimen. In the third status, the impact energy is further than the perforation threshold energy and in this condition impactor after penetration goes across the specimen. In perforation, the magnitude of absorbed energy is less than impact energy and the energy point is located under the equal energy line similar to the rebounding status. A typical equal energy diagram is shown in Fig. 4.

In this diagram, the results of five specimens exposed to low-velocity impacts with different energy levels are presented. As mentioned, the first and second energy points are located under the equal energy line, which causes the impactor to rebound from the surfaces of specimens. Point 3 is located on the equal energy line. Hence, penetration occurs at this energy level. At point 4, the impactor

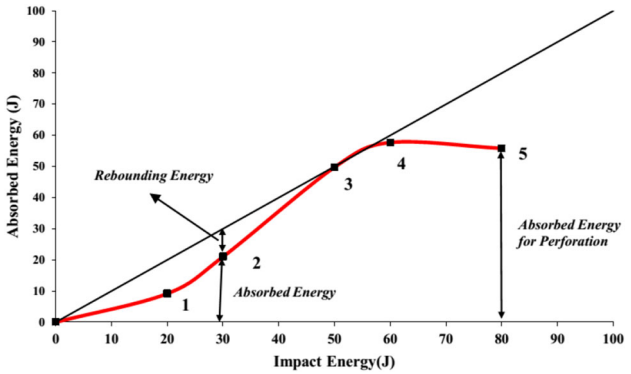

Fig. 4 Typical equal energy diagram

penetrates into the specimen and perforation occurs at this energy level. At point 5, impactor continues its movement after perforating the sample, and wastes remained energy.

This diagram allows determining the appropriate energy magnitude. In order to evaluate the impact results, some characteristics such as maximum load, maximum deflection, absorbed energy, maximum velocity of the impactor and contact duration time should be introduced. Maximum load is the greatest magnitude of contact force that is applied to specimen during impact test. The magnitude of maximum load is measured by force transducer and recorded by the software. Absorbed energy is the magnitude of energy that is absorbed by specimen during damage formation in its structure due to impact. Maximum velocity is the greatest magnitude of impactor velocity during impact test that occurs instantly at the contact time. Under rebounding and perforation conditions, the contact duration time is the total contact time between the impactor and specimen that starts when impactor contacts the specimen and finishes when the impactor leaves the specimen. Analyzing these characteristics is very important for the evaluation of impact behavior of the composite materials.

The specimens from each type of the fabricated composites were exposed to impact with energies up to the penetration then perforation occurs. The data obtained from these tests were used for plotting the energy diagram of the material. The contact load–deflection diagrams for various energies are given in Fig. 5.

In most of the specimens that were tested, the magnitude of impact energy was not enough for penetration of impactor into test specimen and the impactor after collision with the surface of the specimen gave some of its impact energy to test specimen and then changed movement direction. This condition is named as rebounding and in this condition impactor soared after contact with rebounding energy, which is equal to difference of impact energy (E_a) and absorbed energy (E_i). As seen in Fig. 5, the magnitude of impact energy of 20 J is not enough for the penetration of impactor into specimen in all of the materials, hence the rebounding occurred. In this energy magnitude, the maximum contact force is limited to 8039, 5995 and 9530 kN for CFRPs, BFRPs and CBFRPs, respectively. Combination of the high mechanical properties of carbon fiber with good toughness of basalt fiber causes the peak load in the intra-ply CBFRP composites to increase. When the magnitude of impact energy increased to 60 J, the penetration occurred in CFRPs while the rebounding took place for other composite types. The penetration in CFRPs in the low impact energy levels occurred due to low toughness of carbon fiber as well as weakness of these fibers against impact loads (Sarasini et al. 2014). High toughness of basalt fibers and addition of these fibers to the polymer composites leads to this phenomenon (Subagia et al. 2014). At the impact energy of 80 J, the perforation occurred in CFRPs while in the other composite types the impactor rebounded from the surface of the specimen. As shown in Fig. 5, the maximum contact loads are 9.29, 12.64 and 14.12 kN, respectively, for CFRP, BFRP and CBFRP for the impact energy of 80 J. Two important results were obtained from the comparison of the maximum contact loads for 20 and 80 J impact energy. First, the magnitude of contact load was increased due to the increasing impact energy. Second, the higher contact load in CBFRP rather than other composites was repeated in impact energy level of 80 J, similar to that of 20 J. It is concluded that, for all of the impact energy magnitudes, the highest maximum contact load was observed for CBFRPs intra-ply hybrid composites and diagrams of BFRPs were the lowest. Furthermore, most of the contact load–deflection variations are related to initiation of cracks in CFRPs structure during loading. According to Fig. 5, the failure mode in the low energy impact is started with cracking of matrix. By increasing energy magnitude, the failure mode changed to delamination (Sjoblom and Hartness 1988) and as seen in Fig. 5 after delamination, principle failure occurs in the structure of composites (Hosur 2005). Detection of delamination before failure is possible by evaluation of the SEM results or algorithm-based methods (Mohebbi et al. 2013). The energy–time diagrams for the tested specimen are shown in Fig. 6.

Figure 6a shows that the magnitude of rebounding energy is maximum for hybrid composites when the impact energy is 20 J. When the impact energy increases to 50 J, the total energy of the impactor is absorbed by specimen in CFRPs. This phenomenon shows that the penetration occurred in these types of composites (Icten et al. 2009). At the impact energy of 60 J, it seems that the magnitude of absorbed energy for CFRP is higher than that of 60 J. It is understood that this event arose from the potential energy that changes to kinetic energy during fall out of impactor and causes impact energy to increase to approximately

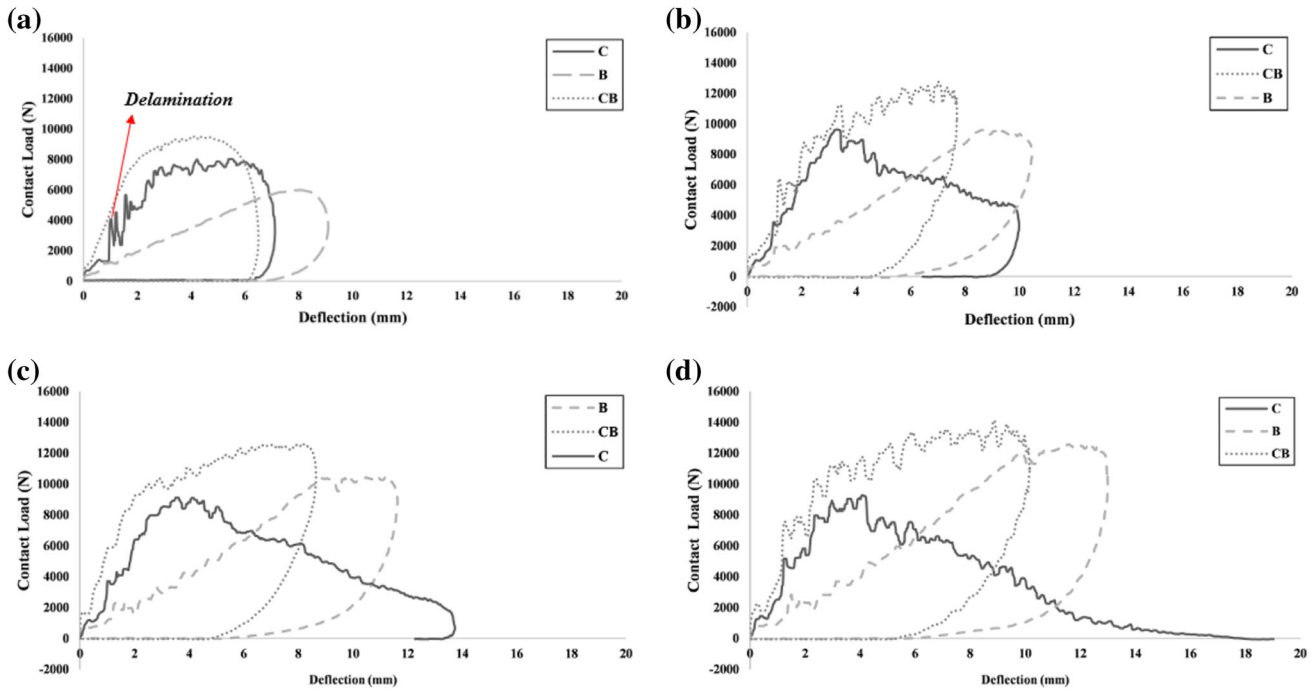

Fig. 5 Contact load–deflection diagrams of homogenous carbon, basalt and intra-ply hybrid of carbon–BFRPs for various impact energy, **a** 20 J, **b** 50 J, **c** 60 J, **d** 80 J

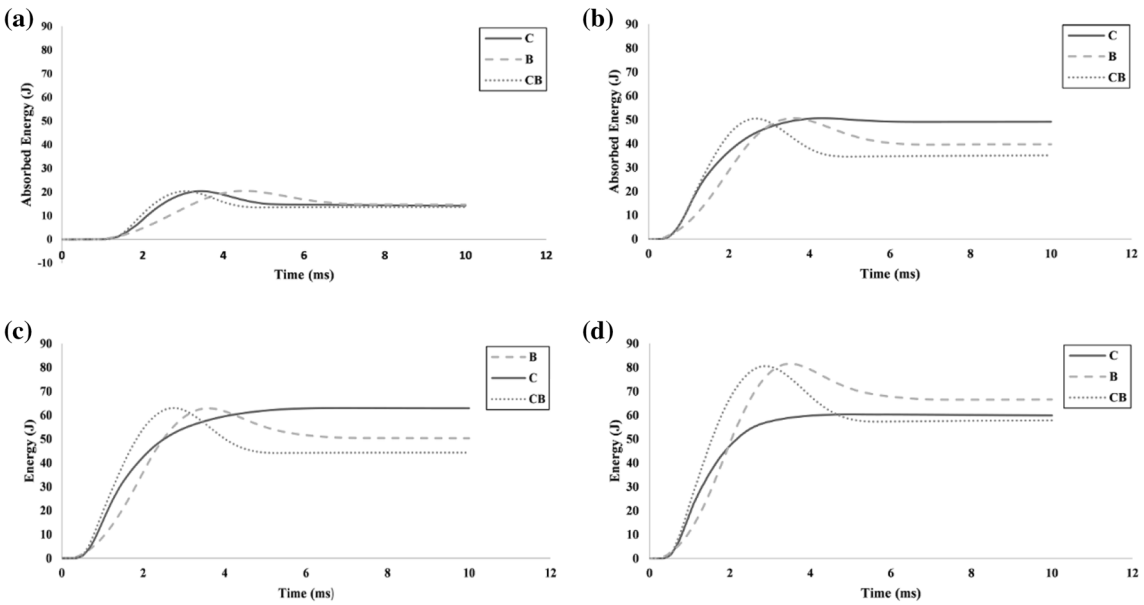

Fig. 6 Energy–time diagrams of homogenous carbon, basalt and intra-ply hybrid of carbon-BFRPs for various impact energy, **a** 20 J, **b** 50 J, **c** 60 J, **d** 80 J

63 J. For the impact energy of 80 J, the absorbed energy by CFRPs is approximately constant at 60 J. This energy magnitude may be enough for the perforation of CFRP specimen and the remaining energy as excessive energy turns into kinetic energy during the motion of impactor after perforation of the specimen. The magnitude of excessive energy varies from 15.05 for CFRPs to 11.8 for BFRPs and 1.73 for CBFRPs. It is shown that addition of the basalt fibers to the structure of the CFRPs causes the energy absorption to increase due to the high potential of basalt fibers in the absorption of energy arising from their high toughness. It is observed that, by enhancing the impact energy, the magnitude of absorbed energy by the tested specimen has increased while the rebounding energy

has decreased. The equal energy diagrams for carbon and basalt fibers and CBFRPs intra-ply hybrid composites are shown in Fig. 7.

Figure 7 depicts that the rebounding occurs up to the impact energy of 60 J for CFRPs with the increasing impact energy. At 60 J and above, the impactor penetrated into the specimen and perforation occurred. For BFRPs, the perforation energy enhances to 100 J because of high toughness of the basalt fiber and good performance of this fiber type against impact loads. According to the equal energy diagram of CBFRPs intra-ply hybrid composites, the penetration occurs at 140 J, whereas the impactor energy was not enough for the perforation that occurred at the energy magnitude above 140 J. It is reasoned that the high perforation energy of intra-ply hybrid composites was due to high mechanical properties of carbon fibers and toughness of basalt fibers. It should be noted that, in the equal energy diagram, the nonlinearity of profiles is not important. The profiles are plotted from connection of limited energy points for each material.

As seen in Fig. 8, the impact peak loads of fabricated composites increase with enhancing the impact energy. The linearity of diagrams up to 20 J, as the impact energy level, is quite obvious and in this region the CBFRPs have the highest peak load value while the BFRPs have the lowest. Beyond 20 J, the linear state of diagrams changes to parabolic curve till 60 J for CFRP, 100 J for BFRP and 140 J for CBFRP in which the penetration occurs and the parabolic diagram turns back to the horizontal state. The horizontal states of the curves at the high-energy level show that the magnitude of peak load remained constant after the perforation. The peak load, maximum duration time, maximum absorbed energy and maximum deflection for 80 J are compared for the fabricated materials in Fig. 10. Also, the impact key parameters of the CBFRP intra-ply hybrid composites for 80 J impact energy are given in Table 2.

The maximum deflection diagrams versus impact energy for all the fabricated composite materials are presented in Fig. 9. Except 20 J, at all of the impact energy levels,

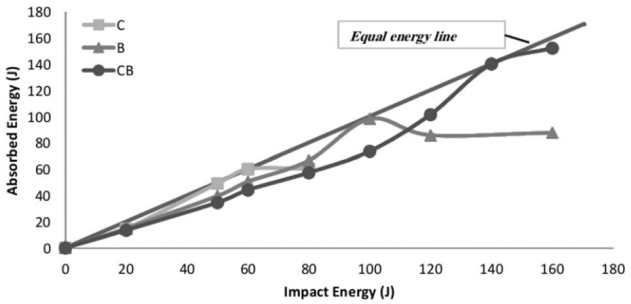

Fig. 7 Equal energy diagram of CFRP, BFRP and CBFRP intra-ply hybrid composites

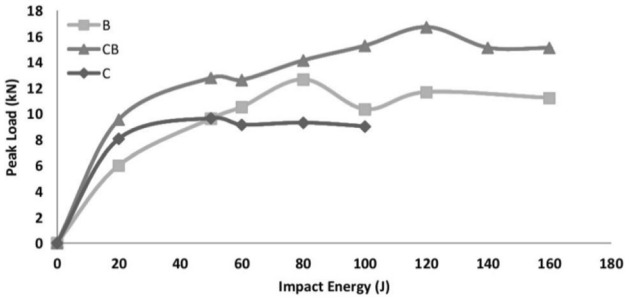

Fig. 8 Peak load versus impact energy diagram of carbon, basalt and CBFRPs intra-ply hybrid composites

CFRPs have the lowest deflections, while for the other impact energies BFRPs have the highest deflection values. High toughness of the basalt fibers may be the main reason of this phenomenon. The deflection value of CBFRPs is located between the deflections of CFRPs and BFRPs. As shown in Fig. 7, the maximum deflection in CFRP, BFRP and CBFRP samples had grown with increasing of the impact energy up to the perforation energy. After this point, the deflection values of all samples remain quite constant. This shows that the amount of damage does not change seriously after the perforation point and the enhancing of impact energy does not affect the damage magnitude. Evaluation of impact damage was carried out accounting for damage degree (equal to E_a/E_i). This parameter that was defined as the ratio of the absorbed energy to the impact energy, before penetration occurrence is less than one and when penetration occurs is equal to one (Shim and Yang 2005). Damage degree is the factor that indicates intensity of damage that occurs in the structure of material due to impact. The magnitudes of damage degree for tested samples are given in Table 2.

According to Fig. 10a, the peak load of CFRP homogenous composites increased 62.98% by intra-ply hybridization of carbon fibers with basalt fibers because of the high toughness of basalt fibers. The effects of hybridization on the contact duration time are illustrated in Fig. 10b. According to the results, this parameter has increased 2.77% by the hybridization of carbon and basalt fibers. The maximum absorbed energy magnitudes during the low-velocity impact test for fabricated homogenous and intra-ply hybrid composites are shown in Fig. 10c. According to these diagrams, the absorbed energy of CFRP decreased approximately 4.37% due to the hybridization with basalt fiber. This phenomenon may be due to the high impact toughness of the CBFRP compared to the CFRP composites. Similar to the other parameters as shown in Fig. 10d, the intra-ply hybridization of carbon and basalt fibers has caused 64.78% increase in the maximum deflection magnitude. The back and front side views of the

Table 2 The key parameters of low-velocity impact for 80 J energy for CFRP, BFRP and CBFRP

Material	Max. force (kN)	Max. deflection (mm)	Max. velocity (m/s)	Absorbed energy (J)	Contact duration time (MS)	Damage degree
CFRP	9.29	5.84	4.88	60.1	3.25	0.751
BFRP	11.66	12.13	5.55	66.76	2.42	0.556
CBFRP	15.08	9.64	6.77	57.47	3.34	0.359

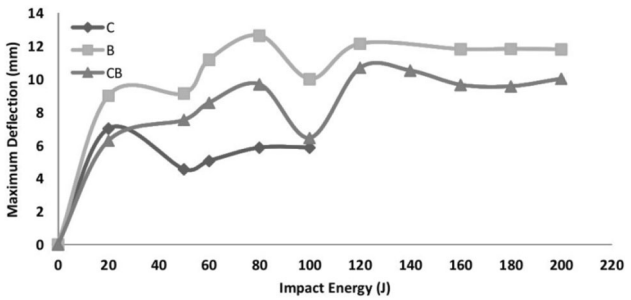

Fig. 9 Maximum deflection versus impact energy diagram of carbon, basalt and CBFRPs intra-ply hybrid composites

perforated CFRP, BFRP and CBFRP samples at 80, 120 and 160 J energy levels are presented in Fig. 11.

The damaged shapes in the front side of the CFRP and the BFRP twill-woven composite have been observed as circular form as shown in Fig. 11. When the diameter of the circular damaged area is measured, it is shown that the diameter of this region was the same as the impactor diameter. Furthermore, not only are cross-shaped cracks and debonding observable in the front surface of BFRPs but also splitting without significant penetration is visible in the back side of this sample. It is noticed that fiber breakage is the dominant damage mode in the CFRPs while matrix breakage is dominant in the BFRPs. In the CBFRPs, damage shapes are ellipsoidal and it is seen that the fiber and matrix breakage have occurred together during the perforation.

Fiber pull out caused by weak adhesion of matrix and fibers, fiber breakage due to high through-thickness stresses, matrix cracking due to through-thickness shear stresses and delamination caused by mode II inter-laminar shear

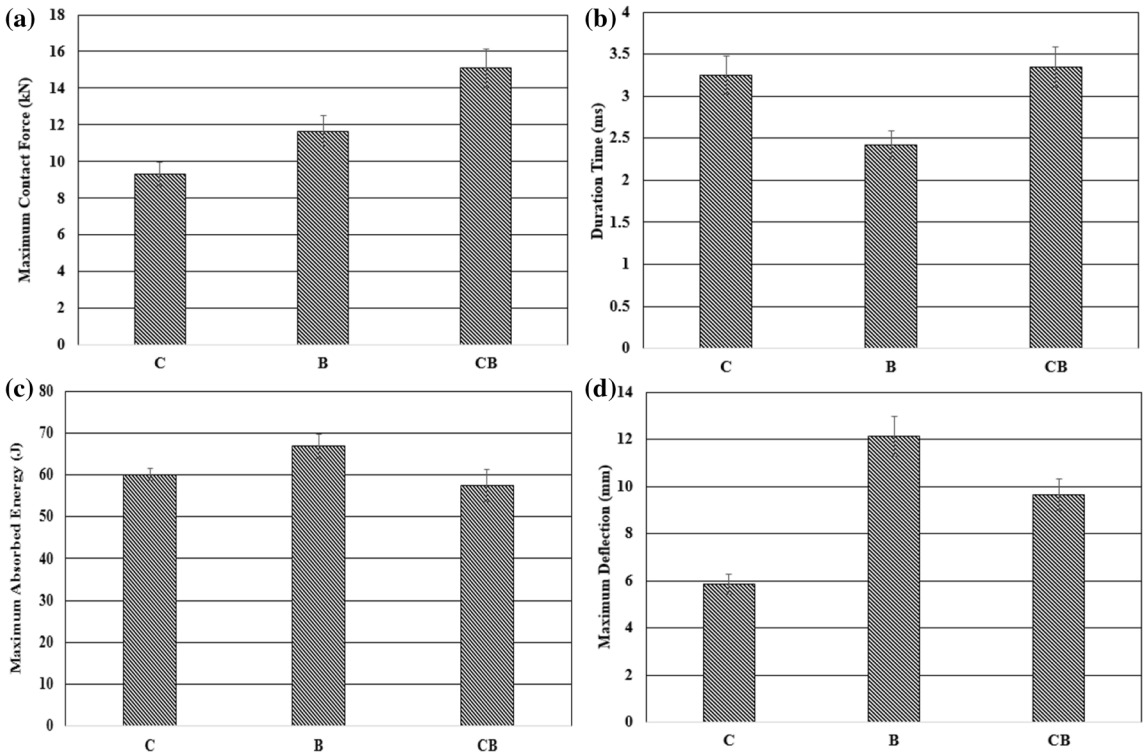

Fig. 10 Comparison of low-velocity impact parameters for CFRP, BFRP and CBFRP, **a** peak load, **b** maximum duration time, **c** maximum absorbed energy, **d** maximum deflection

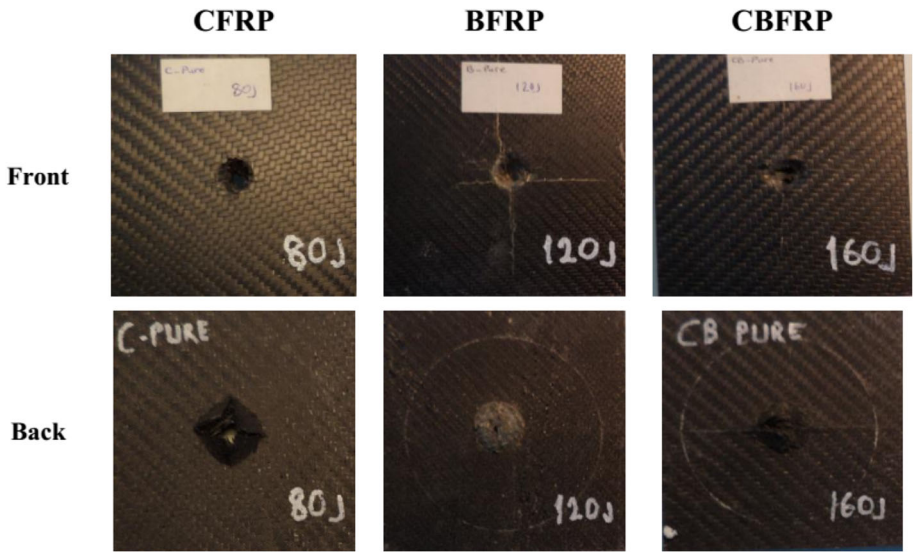

Fig. 11 Front and back side of perforated samples

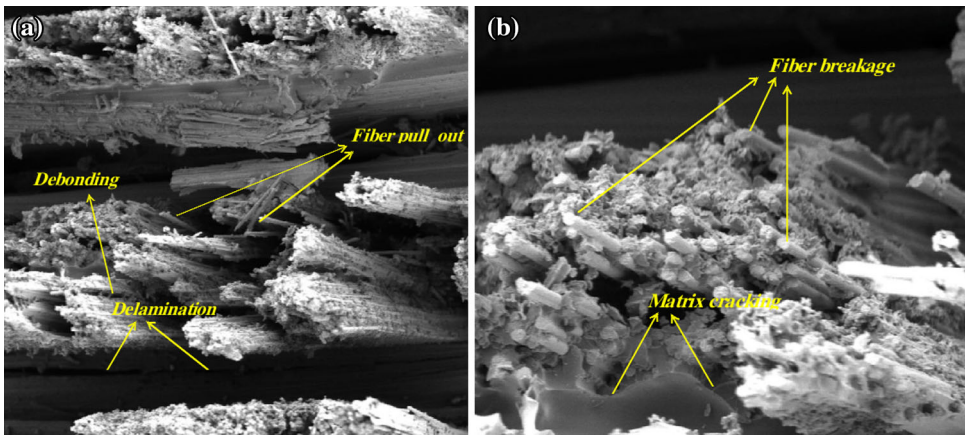

Fig. 12 Microstructural failure mechanisms of CBFRP composites due to low-velocity impact

stresses generated by the bending of the laminate are the important failure mechanisms observed in the SEM results of damaged samples (Fig. 12a, b).

4 Conclusion

The effects of intra-ply hybridization on the low-velocity impact behavior of carbon and basalt-based composites were investigated. It is concluded that the CFRPs, because of low toughness of the carbon fibers, showed weak performance against low-velocity impact and were perforated at 80 J impact energy. The hybridization of carbon fiber with basalt fiber may be offered as a solution of this problem, which leads to the improvement in CFRP toughness because of high toughness of the basalt fibers. It is observed that the load–deflection diagram of the BFRPs is smoother when compared to other composites because of high toughness of the basalt fibers that leads to soft penetration of impactor into these materials. The magnitude of absorbed energy in intra-ply CBFRP is lower than those of other materials. Hence, the damage rate remains small in this material. Another important result is that the size of damage did not change severely followed by the perforation with the increasing impact energy. The same peak load remained almost constant after the perforation point and was not seriously altered. Among the fabricated materials, the CBFRPs have shown the maximum peak load, the contact duration time and the absorbed energy while the maximum deflection and the damage was observed in BFRPs. Thereupon, the intra-ply hybridization of the carbon fibers with basalt fibers has improved the impact behavior of CFRPs. Furthermore, the fiber breakage became dominant damage mode in the CFRPs while the matrix damage is dominant in the BFRPs. However, the damage mode for the CBFRPs is represented in the form of the mixture of fiber and matrix breakage.

Acknowledgements The authors would like to gratefully acknowledge the financial support provided by the Scientific and Technological

Research Council of Turkey (TUBITAK), Project No. 213M600 and Ataturk University Scientific Research Grant, BAP 2012/448. Furthermore, the authors would like to thank Dr. Özgür Seydibeyoğlu and Ph.D. candidate Volkan Acar for their contributions.

References

Akangah P, Lingaiah S, Shivakumar K (2010) Effect of Nylon-66 nano-fiber interleaving on impact damage resistance of epoxy/carbon fiber composite laminates. Compos Struct 92:1432–1439. https://doi.org/10.1016/j.compstruct.2009.11.009

Carmisciano S, De Rosa IM, Sarasini F, Tamburrano A, Valente M (2011) Basalt woven fiber reinforced vinylester composites: flexural and electrical properties. Mater Des 32:337–342. https://doi.org/10.1016/j.matdes.2010.06.042

Chandekar GS, Kelkar AD (2014) Experimental and numerical investigations of textile hybrid composites subjected to low velocity impact loadings. Sci World J 2014(2014). https://doi.org/10.1155/2014/325783

Czigany T (2006) Special manufacturing and characteristics of basalt fiber reinforced hybrid polypropylene composites: mechanical properties and acoustic emission study. Compos Sci Technol 66:3210–3220. https://doi.org/10.1016/j.compscitech.2005.07.007

Fiore V, Di Bella G, Valenza A (2011) Glass–basalt/epoxy hybrid composites for marine applications. Mater Des 32(4):2091–2099

Fiore V, Scalic T, Di Bella G (2015) A review on basalt fibre and its composites. Compos Part B: Eng 74:74–94

Han SH, Oh HJ, Lee HC, Kim SS (2013) The effect of post-processing of carbon fibers on the mechanical properties of epoxy-based composites. Compos B Eng 45:172–177. https://doi.org/10.1016/j.compositesb.2012.05.022

Hosur MV (2005) Studies on the low-velocity impact response of woven hybrid composites. Compos Struct 67:253–262

Icten BM, Atas C, Aktas M, Karakuzu R (2009) Low temperature effect on impact response of quasi-isotropic glass/epoxy laminated plates. Compos Struct 91:318–323

Imielinska K, Guillaumat L (2004) The effect of water immersion ageing on low-velocity impact behaviour of woven aramid-glass fibre/epoxy composites. Compos Sci Technol 64:2271–2278. https://doi.org/10.1016/j.compscitech.2004.03.002

Karahan M, Karahan N (2014) Effect of weaving structure and hybridization on the low-velocity impact behavior of woven carbon-epoxy composites. Fibres Text East Eur 3(105):109–115

Kumar CS, Arumugam V, Dhakal HN, John R (2015) Effect of temperature and hybridisation on the low velocity impact behavior of hemp-basalt/epoxy composites. Compos Struct 125:407–416

Liu Q, Shaw MT, Parnas RS, McDonnell AM (2006) Investigation of basalt fiber composite mechanical properties for applications in transportation. Polym Compos 27:41–48. https://doi.org/10.1002/Pc.20162

Mcconnell EE, Kamstrup O, Musselman R, Hesterberg TW, Chevalier J, Miiller WC, Thevenaz P (1994) Chronic inhalation study of size-separated rock and slag wool insulation fibers in Fischer 344/N rats. Inhal Toxicol 6:571–614. https://doi.org/10.3109/08958379409003042

Mohebbi B, Abbasidoust F, Ettefagh MM, Biglari H (2013) Delamination diagnosis in composite beam using AIS and BGA algorithms based on vibration characteristics. Adv Struct Mater 43:73–89

Muñoz R, Delgado S, González C, López-Romano B, Wang D-Y, LLorca J (2014) Modeling lightning impact thermo-mechanical damage on composite materials. Appl Compos Mater 21:149–164

Nayak SK, Mohanty S, Samal SK (2009) Influence of short bamboo/glass fiber on the thermal, dynamic mechanical and rheological properties of polypropylene hybrid composites. Mater Sci Eng A Struct 523:32–38. https://doi.org/10.1016/j.msea.2009.06.020

Pegoretti A, Fabbri E, Migliaresi C, Pilati F (2004) Intraply and interply hybrid composites based on E-glass and poly(vinyl alcohol) woven fabrics: tensile and impact properties. Polym Int 53:1290–1297. https://doi.org/10.1002/Pi.1514

Petrucci R, Santulli C, Puglia D, Sarasini F, Torre L, Kenny JM (2013) Mechanical characterisation of hybrid composite laminates based on basalt fibres in combination with flax, hemp and glass fibres manufactured by vacuum infusion. Mater Des 49:728–735. https://doi.org/10.1016/j.matdes.2013.02.014

Ramachandran BE, Velpari V, Balasubramanian N (1981) Chemical durability studies on basalt fibers. J Mater Sci 16:3393–3397. https://doi.org/10.1007/Bf00586301

Rosa IMD, Marra F, Pulci G, Santulli C, Sarasini F, Tirillò J, Valente M (2012) Post-impact mechanical characterisation of glass and basalt woven fabric laminates. Appl Compos Mater 19:475–490

Rout J, Misra M, Tripathy SS, Nayak SK, Mohanty AK (2001) The influence of fibre treatment on the performance of coir-polyester composites. Compos Sci Technol 61:1303–1310. https://doi.org/10.1016/S0266-3538(01)00021-5

Sarasini F, Tirillò J, Valente M, Ferrante L, Cioffi S, Iannace S (2013a) Hybrid composites based on aramid and basalt woven fabrics: impact damage modes and residual flexural properties. Mater Des 49:290–302

Sarasini F, Tirillò J, Valente M, Valente T, Cioffi S, Iannace S, Sorrentino L (2013b) Effect of basalt fiber hybridization on the impact behavior under low impact velocity of glass/basalt woven fabric/epoxy resin composites. Compos A 47:109–123

Sarasini F et al (2014) Drop-weight impact behaviour of woven hybrid basalt-carbon/epoxy composites. Compos B Eng 59:204–220. https://doi.org/10.1016/j.compositesb.2013.12.006

Shim V, Yang L (2005) Characterization of the residual mechanical properties of woven fabric reinforced composites after low-velocity impact. Int J Mech Sci 47:647–665

Sim J, Park C, Moon DY (2005) Characteristics of basalt fiber as a strengthening material for concrete structures. Compos B Eng 36:504–512. https://doi.org/10.1016/j.compositesb.2005.02.002

Sjoblom PO, Hartness T (1988) On low-velocity impact testing of composite materials. Mater Sci Compos 22(1):30–52

Subagia IDGA, Kim Y, Tijing LD, Kim CS, Shon HK (2014) Effect of stacking sequence on the flexural properties of hybrid composites reinforced with carbon and basalt fibers. Compos B Eng 58:251–258. https://doi.org/10.1016/j.compositesb.2013.10.027

Szabo JS, Czigány T (2003) Static fracture and failure behavior of aligned discontinuous mineral fiber reinforced polypropylene composites. Polym Test 22(6):711–719

Tehrani-Dehkordi M, Nosraty H, Rajabzadeh MH (2015) Effects of plies stacking sequence and fiber volume ratio on flexural properties of basalt/nylon-epoxy hybrid composites. Fiber Polym 16:918–925. https://doi.org/10.1007/s12221-015-0918-8

Wei B, Cao HL, Song SH (2010) Tensile behavior contrast of basalt and glass fibers after chemical treatment. Mater Des 31:4244–4250. https://doi.org/10.1016/j.matdes.2010.04.009

Wei B, Cao HL, Song SH (2011) Degradation of basalt fibre and glass fibre/epoxy resin composites in seawater. Corros Sci 53:426–431. https://doi.org/10.1016/j.corsci.2010.09.053

Zhang Q, Liu J, Sager R, Dai L, Baur J (2009) Hierarchical composites of carbon nanotubes on carbon fiber: influence of growth condition on fiber tensile properties. Compos Sci Technol 69:594–601